Ina Remy-Speckmann, Thomas Bredow, Martin Lerch

Two new quaternary copper bismuth sulfide halides: CuBi2S3Cl and CuBi2S3Br as candidates for copper ion conductivity

Contribution to Special Issue dedicated to Paul Heitjans

Ina Remy-Speckmann, Thomas Bredow and Martin Lerch*

Two new quaternary copper bismuth sulfide halides: $CuBi_2S_3Cl$ and $CuBi_2S_3Br$ as candidates for copper ion conductivity

https://doi.org/10.1515/zpch-2021-3120
Received August 31, 2021; accepted September 30, 2021; published online October 14, 2021

Abstract: Two new copper bismuth sulfide halides, $CuBi_2S_3Cl$ and $CuBi_2S_3Br$, were synthesized by a two-step process of ball milling followed by annealing. Both compounds are obtained as dark grey powders and crystallize in the monoclinic space group $C2/m$ with lattice parameters a = 12.9458(11) Å, b = 3.9845(3) Å, c = 9.1024(8) Å and β = 91.150(3)° for the sulfide chloride and a = 13.3498(8) Å, b = 4.1092(2) Å, c = 9.4173(6) Å and β = 90.322(4)° for the sulfide bromide. Also known for related compounds, the copper atoms are strongly disordered. Quantum-chemical calculations suggest that modelling the structure with fixed copper positions does not satisfactorily describe all structural features, which insinuates copper ion mobility at elevated temperatures.

Keywords: bismuth; copper; mechanochemical synthesis; quantum-chemical calculations; Rietveld refinement; sulfide halide.

1 Introduction

The research area on quaternary compounds in the system M/Bi/Q/X, with M = copper or silver, Q = sulfide or selenide, and X = chlorine, bromine or iodine, was predominantly developed in the last years. Various compounds containing

Dedicated to: *Professor Paul Heitjans on the occasion of his 75th birthday.*

***Corresponding author: Martin Lerch**, Institut für Chemie, Technische Universität Berlin, Straße des 17. Juni 135, 10623 Berlin, Germany, E-mail: martin.lerch@tu-berlin.de
Ina Remy-Speckmann, Institut für Chemie, Technische Universität Berlin, Straße des 17. Juni 135, 10623 Berlin, Germany
Thomas Bredow, Mulliken Center for Theoretical Chemistry, Institut für Physikalische und Theoretische Chemie, Universität Bonn, Beringstraße 4, 53115 Bonn, Germany

silver [1–5] and copper [5–13] were synthesized and published by Ruck and coworkers, only a few copper-containing examples are described by other scientists [14–17]. Several of the published copper compounds exhibit the same structural feature: copper cations cannot be assigned to a certain, fully occupied position. Instead, the voids within a rigid framework of bismuth, chalcogenide and halide atoms are partly occupied by highly disordered copper atoms [8–14, 17]. This disorder suggests a high mobility of the copper cations at elevated temperatures and therefore qualifies these compounds as candidates for ionic conduction [9, 11, 14]. In this paper, we present two new members of the family of copper bismuth sulfide halides, $CuBi_2S_3Cl$ and $CuBi_2S_3Br$.

2 Results and discussion

2.1 Experimental results

The two new sulfide halides, $CuBi_2S_3Cl$ (**1**) and $CuBi_2S_3Br$ (**2**), were synthesized mechanochemically from bismuth sulfide and the corresponding copper halides. Following the mechanochemical process, both samples were annealed at elevated temperatures. Temperatures higher than 200 °C led to the decomposition of the desired phases and to the formation of various copper bismuth sulfides. Therefore, the samples could only be annealed at 200 °C and exhibit merely mediocre crystallinity. Both compounds were obtained as dark grey powders. Since the copper halides were stored under an inert atmosphere, milling was also carried out under that atmosphere. However, the annealed products can be handled in air without decomposition. Their composition was confirmed by EDX measurements.

Comparing the powder diffraction patterns of the two sulfide halides with literature data, there is a strong resemblance to a non-stoichiometric copper bismuth sulfide bromide, $Cu_{1.5}Bi_{2.64}S_{3.42}Br_{2.58}$, which crystallizes in space group $C2/m$ [13]. Initial leBail fits using the program Jana2006 [18] for both **1** and **2** point to the fact that they also crystallize in $C2/m$ with similar lattice parameters compared to the non-stoichiometric sulfide bromide. The lattice parameters for the sulfide bromide **2** are slightly larger than those for the sulfide chloride **1**, corresponding to the increase of the ionic radius from chloride to bromide. First attempts to solve the structure of both sulfide halides with the program Superflip [19] implemented in Jana2006 led to the coordinates of the bismuth and anion positions, but showed no positions for the copper atoms. This agrees with the phenomenon already mentioned in the introduction: some members of the Cu/Bi/Q/X family show a rigid body of bismuth, chalcogenide and halide atoms and highly disordered copper atoms in the voids of these frameworks. Therefore, at first only the

framework of bismuth, sulfide and halide atoms was refined, wherein **1** and **2** are isostructural. The bismuth cations occupy two independent positions, *2d* and *4i*. Additionally, there are three independent anion positions, all of them with Wyckoff notation *4i*. Since sulfide and chloride anions cannot be distinguished with conventional X-ray scattering experiments, the anion distribution on the three possible positions was taken from the sulfide bromide compound: starting with a statistical distribution of the anions, the occupation of the three anion positions was refined for compound **2**. The results indicated that only one position is partly occupied with bromide, while the other two are fully occupied with sulfur. The occupancies for the mixed position were set to their ideal values according to the composition. Additionally, the coordinates and Debye-Waller factors were kept identical for sulfide and bromide. The anion distribution for **2** was transferred to the sulfide chloride **1**. After the refinement of the framework reached reasonable *R* values for both compounds, the copper atoms were incorporated into the structure using difference Fourier maps calculated by Jana2006. From these maps, possible coordinates for the copper atoms were derived and added to the atomic model. In both compounds copper occupies a split position. For the sulfide chloride, copper occupies the position *8j*, for the sulfide bromide the *4g* position. The coordinates of the copper atoms were refined for both compounds, but the occupation was set to its ideal value corresponding to the formula of the compound. Also the Debye-Waller factors of the copper atoms were fixed at 0.05 $Å^2$. Literature examples, which are exclusively solved using single crystal diffraction data, usually feature several copper positions with low occupations. However, due to the experimental conditions, only powder diffraction data from samples exhibiting mediocre crystallinity was available. Thus, a more sophisticated modelling of the copper atoms was not reasonable. For example, incorporating more copper positions into the model led to unstable refinements without improving the *R* values. The same behavior was observed refining the occupation factors or Debye-Waller factors of the copper atoms. Consequently, the proposed positions for the copper atoms have to be considered only as a rough approach to the actual structure. In the last refinement cycle, all parameters causing correlations greater than 0.9 were fixed. The final results of the Rietveld refinements [20] of both compounds can be found in Table 1. The graphical results of the refinements with the X-ray diffraction patterns are shown in Figure 1. Wyckoff positions, atomic coordinates and Debye-Waller factors for $CuBi_2S_3Cl$ and $CuBi_2S_3Br$ are depicted in Tables 2 and 3, respectively.

The bismuth atom on Wyckoff position *4i* (Bi1) is coordinated by a bicapped trigonal prism of three mixed anion positions and five sulfur positions. The five sulfur positions are on one side of the prism while the three mixed anion positions are on the other side. Hence, the bismuth atom is slightly deflected from the center

Table 1: Results of the Rietveld refinements for $CuBi_2S_3Cl$ and $CuBi_2S_3Br$.

Empirical formula	$CuBi_2S_3Cl$	$CuBi_2S_3Br$
M_r/g mol^{-1}	613.1	657.6
Color	Dark grey	
Space group	$C2/m$ (no. 12)	
Crystal system	Monoclinic	
Z	3	
a/Å	12.9458(11)	13.3498(8)
b/Å	3.9845(3)	4.1092(2)
c/Å	9.1024(8)	9.4173(6)
β/°	91.150(3)	90.322(4)
V/Å^3	469.43(7)	516.60(5)
ρ_{calc}/g cm^{-3}	6.5066	6.3412
Refined parameters	35	38
Constraints	3	3
R_p, wR_p[b]	0.0328; 0.0442	0.0342; 0.0458
S (all)	3.13	1.93
R_F (obs[a]; all)	0.0664; 0.0664	0.0574; 0.0574
wR_F[b] (obs[a]; all)	0.0913; 0.0913	0.0699; 0.0699
R_B (obs[a])	0.1132	0.1092
$\Delta\rho_b$(min, max)/fm Å^{-3}	−6.47, 2.86	−6.87, 2.65

[a] $I > 3\sigma(I)$. [b] $w = 1/[\sigma^2(I) + (0.01I)^2]$.

of the prism to the side of higher negative anion charge (Figure 3a). These bicapped trigonal prisms form layers perpendicular to the *a* axis by shared faces along the *b* axis and shared edges along the *c* axis (Figure 2, bottom). The second bismuth atom on Wyckoff position *2d* (Bi2) is coordinated octahedrally. The octahedral coordination of Bi2 differs slightly from **1** compared to **2**. Four mixed anion positions form the square base of the octahedron parallel to the *C* plane, while two sulfide anions form the tips of the octahedron along the *c* axis (Figure 2, top). Due to the increased radius of bromide compared to chloride, the bond distances between the bismuth atom and the atoms on the mixed anion positions are slightly larger than those between the bismuth atom and the sulfide anions for the sulfide bromide **2**, whereas all six bond distances are nearly the same for the sulfide chloride **1**. The octahedra form threads parallel to the *b* axis by sharing edges along the *b* axis (Figure 2, top). The threads of octahedrally coordinated bismuth cations and layers of bismuth atoms surrounded by bicapped trigonal prisms are connected by shared edges along the *a* axis.

The copper atoms on the split positions *8j* for **1** and *4g* for **2** partially occupy the octahedral voids generated by the described framework (Figure 2). The octahedral voids show the same structural pattern as the bismuth atoms on position *2d* by

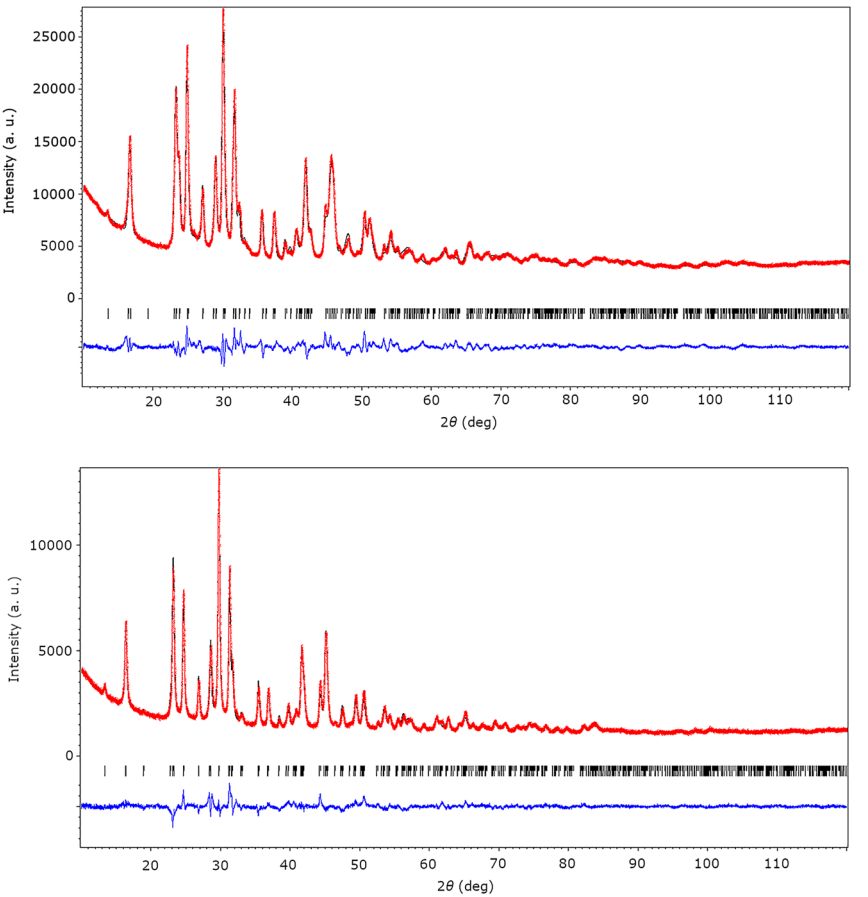

Figure 1: X-ray diffraction patterns and results of the Rietveld refinements for $CuBi_2S_3Cl$ (top) and $CuBi_2S_3Br$ (bottom). Experimental data in red, calculated data in black and difference plots in blue.

Table 2: Wyckoff positions, coordinates and Debye Waller factors for $CuBi_2S_3Cl$ (**1**), standard deviations in parentheses.

Atom	Wyckoff site	*x*	*y*	*z*	s.o.f.	U_{iso} (Å^2)
Bi1	*4i*	0.77672(9)	0	0.80147(2)	1	0.0397(8)
Bi2	*2d*	½	0	½	1	0.0466(11)
S1	*4i*	0.1423(4)	0	0.9503(6)	1	0.017(3)
S2	*4i*	0.4172(5)	0	0.7687(6)	1	0.012
S3	*4i*	0.1358(5)	0	0.5526(6)	0.25	0.034(3)
Cl1	*4i*	0.1358(5)	0	0.5526(6)	0.75	0.034(3)
Cu1	*8j*	0.5132(6)	0.8482(11)	0.9390(6)	0.375	0.05

Table 3: Wyckoff positions, coordinates and Debye Waller factors for $CuBi_2S_3Br$ (**2**), standard deviations in parentheses.

Atom	Wyckoff site	*x*	*y*	*z*	s.o.f.	U_{iso} (Å^2)
Bi1	*4i*	0.77786(13)	0	0.81069(15)	1	0.0201(6)
Bi2	*2d*	½	0	½	1	0.0464(12)
S1	*4i*	0.1440(6)	0	0.9222(10)	1	0.022(4)
S2	*4i*	0.4385(6)	0	0.7716(8)	1	0.012
S3	*4i*	0.1484(4)	0	0.5543(4)	0.25	0.0154(16)
Br1	*4i*	0.1485(4)	0	0.5543(4)	0.75	0.0154(16)
Cu1	*4g*	½	0.8242(14)	0	0.75	0.05

building threads through shared edges along the *b* axis. They are connected to the framework of bismuth polyhedra by sharing edges with the layers of bismuth coordinated by bicapped trigonal prisms and sharing corners with the threads of octahedrally coordinated bismuth atoms. Due to the anion distribution, copper is only coordinated by sulfide anions, an observation also made in other related compounds [11]. With respect to the compositions of the compounds and the multiplicity of the Wyckoff positions, the copper positions are only occupied with 37.5% for **1** and 75% for **2**. An occupation of copper positions with very close distances to each other is therefore not likely.

Two silver-containing compounds with the same principal composition as the herein presented ones, $AgBi_2S_3Cl$ and $AgBi_2Se_3Cl$, crystallize in a different monoclinic space group, $P2_1/m$ [1]. Nonetheless, the structure motives described above can be found in other related compounds such as $AgBiSCl_2$ [5], $CuBiSCl_2$ [5] or $FeBiS_2Cl$ [21], although these compounds crystallize with higher symmetry in space group *Cmcm*. These crystal structures also show the layers of bismuth atoms coordinated by bicapped trigonal prisms and layers of edge-sharing octahedra. But as a consequence of their composition, the bismuth atoms only occupy the positions coordinated by bicapped trigonal prisms and the octahedrally coordinated cation positions are filled with the transition metal cation.

Additionally, the crystal structure of the already mentioned non-stoichiometric copper bismuth sulfide bromide $Cu_{1.5}Bi_{2.64}S_{3.42}Br_{2.58}$ shows a strong resemblance to the herein presented compounds, especially to the sulfide bromide **2**. However, due to the different composition and therefore altered anion distribution, the structures differ slightly. The non-stoichiometric compound, $Cu_{1.5}Bi_{2.64}S_{3.42}Br_{2.58}$, can be seen as a member of the pavonite homologous series [13]. The pavonite structure type contains two alternating modules *A* and *B* [3]. While *A* is formed from paired capped trigonal prisms alternating with

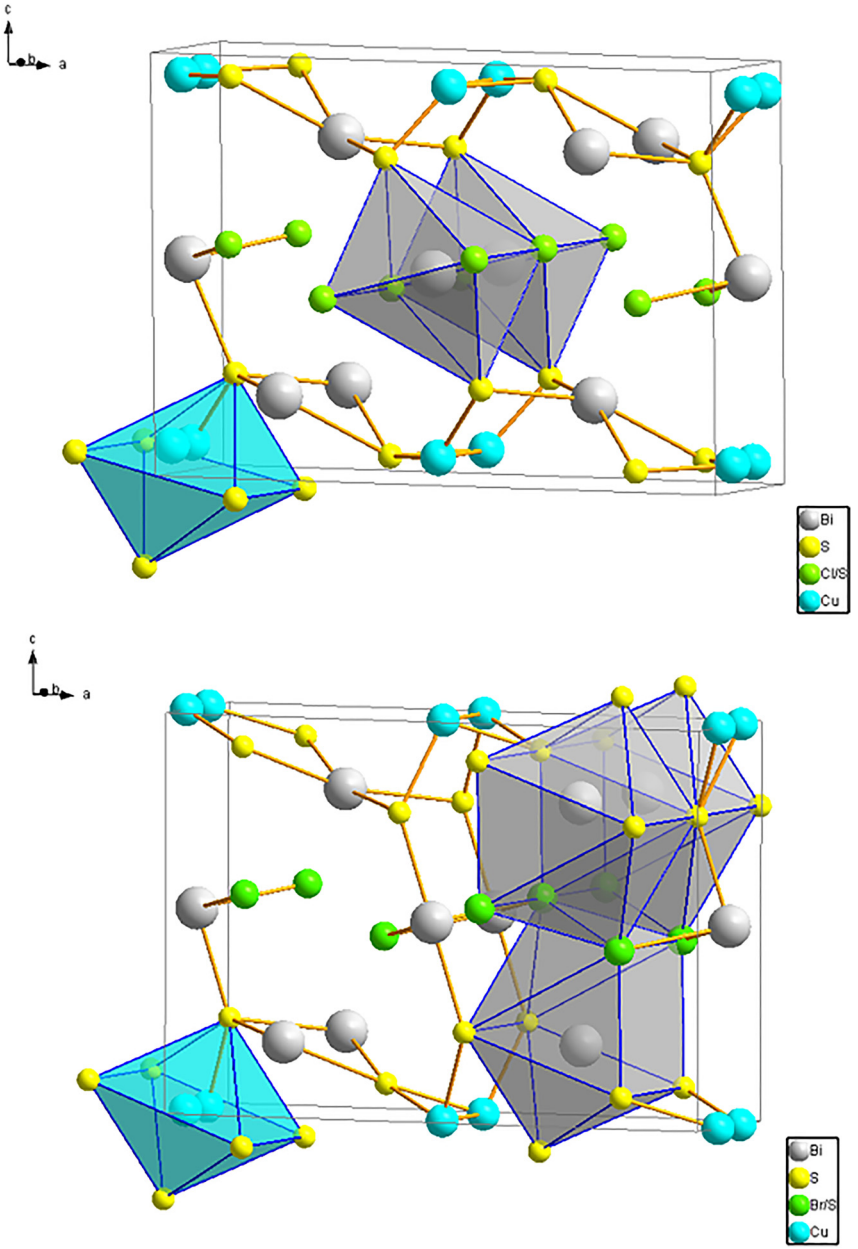

Figure 2: Crystal structures of $CuBi_2S_3Cl$ (top) with coordination of Bi2 (grey octahedra) and $CuBi_2S_3Br$ (bottom) with coordination of Bi1 (grey polyhedra). Octahedral voids occupied by copper in both structures are shown in light blue.

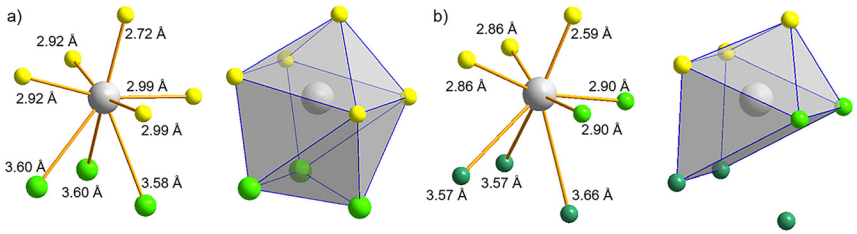

Figure 3: Bismuth atom on position *4i* (grey) and its coordinating anions, sulfide in yellow, mixed anion position in green, bromide in petrol, with the corresponding bond distances (left) and coordination polyhedra (right) for a) $CuBi_2S_3Br$ and b) $Cu_{1.5}Bi_{2.64}S_{3.42}Br_{2.58}$ [13].

octahedrally coordinated cations, *B* holds chains of edge sharing octahedra. Depending on the number of octahedra *N* stacked along the *c* axis, the *B* module can grow along the *c* axis. The non-stoichiometric copper bismuth sulfide halide can therefore be classified as a member of the pavonite series with $N = 1$ [13]. The difference between the structures belonging to the pavonite series and the herein presented structures is the coordination of the bismuth atom Bi1. In the crystal structures **1** and **2**, the bond lengths between atoms on the mixed anion position forming one cap of the trigonal prism and the central bismuth atom are shorter than those between the central bismuth atom and the atoms on the other two mixed anion positions that form one edge of the trigonal prism (Figure 3a). Therefore, all mixed anion positions have to be considered for coordination. In compounds belonging to the pavonite series, the trigonal prism surrounding the bismuth atom is not bicapped. The lower right bromide position in Figure 3b has a larger distance to the central bismuth atom than the other two bromide positions. Therefore, the lower right bromide position is not included into the coordination polyhedron, resulting in a monocapped trigonal prismatic coordination for the bismuth atom. Thus, the compounds **1** and **2** show a close relation to the pavonite series, but can rather be interpreted as related to the above-mentioned quaternary bismuth sulfide halides.

2.2 Quantum-chemical calculations

The experimentally suggested crystal structures of **1** and **2** shown in Tables 1–3 were used as starting points for periodic quantum-chemical calculations at density-functional theory (DFT) level. All atom positions were fully relaxed without symmetry restrictions, while the lattice parameters were kept fixed. Test calculations where the lattice parameters were also allowed to relax showed large

deviations from the measured values. For $Cu_3Bi_6S_9Cl_3$ a = 12.916 Å, b = 3.971 Å, c = 9.295 Å, and β = 90.6° were obtained. These values deviate by −0.2, −0.3, +2.1 and −0.6% from experiment. Similar deviations were observed for $Cu_3Bi_6S_9Br_3$ (a = 12.961 Å, b = 4.105 Å, c = 9.327 Å, and β = 89.1°; deviations: −3.6, −0.1, −1.0, −1.4%). The deviations are depending on the cation and anion distribution (see below). We therefore decided not to optimize the lattice parameters in the following. Initially the effect of S3/Cl1 or Br1 distribution on the lattice energy was checked by placing a sulfur atom on one of the four *4i* Wyckoff sites. No significant changes in total energy were observed. The fractional occupation of the suggested Cu *8j* (*4g*) Wyckoff sites was modeled by removing five (one) of eight (four) copper atoms in the conventional unit cell, respectively. The remaining copper atoms were selected on the basis of their interatomic distances. If all *8j* (*4g*) positions are occupied, unreasonably short Cu-Cu distances of ~1.2 (1.2) Å are present. The shortest Cu-Cu distances of the selected structures are ~1.7 Å, respectively, before optimization. The stoichiometry of the cells was $Cu_3Bi_6S_9X_3$ with X = Cl, Br. During structure relaxation, one copper atom moves by ~1.5 Å in order to increase the Cu-Cu

Table 4: Optimized atomic positions (space group no. 6) of $CuBi_2S_3Cl$ (**1**).

Atom	Wyckoff site	*x*	*y*	*z*
Bi1	*1a*	0.20012	0.00000	0.72270
Bi2	*1b*	0.21054	0.50000	0.22751
Bi3	*1a*	0.82201	0.00000	0.25983
Bi4	*1b*	0.80796	0.50000	0.78547
Bi5	*1b*	0.49660	0.50000	0.48705
Bi6	*1a*	0.51361	0.00000	−0.00126
S1	*1a*	0.07291	0.00000	0.35960
S2	*1b*	0.07429	0.50000	0.86419
S3	*1a*	−0.07270	0.00000	0.66395
S4	*1b*	−0.05818	0.50000	0.14596
S5	*1b*	0.22042	0.50000	0.58076
S6	*1a*	0.23343	0.00000	0.08418
S7	*1b*	0.78534	0.50000	0.42781
S8	*1a*	0.78988	0.00000	−0.06264
S9	*1a*	0.44813	0.00000	0.35365
Cl1	*1b*	0.44736	0.50000	0.85600
Cl2	*1a*	0.56521	0.00000	0.65340
Cl3	*1b*	0.56619	0.50000	0.14443
Cu1	*1b*	0.04341	0.50000	0.46027
Cu2	*1a*	0.04203	0.00000	−0.02734
Cu3	*1a*	0.85242	0.00000	0.50129

Table 5: Optimized atomic positions (space group no. 6) of $CuBi_2S_3Br$ (**2**).

Atom	Wyckoff site	*x*	*y*	*z*
Bi1	*1a*	0.18946	0.00000	0.71115
Bi2	*1b*	0.20143	0.50000	0.21853
Bi3	*1a*	0.83186	0.00000	0.27142
Bi4	*1b*	0.81844	0.50000	0.79005
Bi5	*1b*	0.49500	0.50000	0.48101
Bi6	*1a*	0.52080	0.00000	0.00207
S1	*1a*	0.07598	0.00000	0.36075
S2	*1b*	0.07484	0.50000	0.86149
S3	*1a*	−0.07651	0.00000	0.66374
S4	*1b*	−0.06175	0.50000	0.15474
S5	*1b*	0.21561	0.50000	0.57622
S6	*1a*	0.22802	0.00000	0.08128
S7	*1b*	0.78876	0.50000	0.43378
S8	*1a*	0.79200	0.00000	−0.06482
S9	*1a*	0.44948	0.00000	0.35600
Br1	*1b*	0.44975	0.50000	0.85776
Br2	*1a*	0.56204	0.00000	0.65000
Br3	*1b*	0.56691	0.50000	0.15318
Cu1	*1b*	0.04477	0.50000	0.45713
Cu2	*1a*	0.04563	0.00000	−0.03268
Cu3	*1a*	0.84845	0.00000	0.50402

distance to ~2.8 Å. All other atoms relax by only a few tenths of an Å. For both compounds **1** and **2** the optimizations starting from copper on either *8j* and *4g* positions converged to similar structures. Symmetry analysis with FINDSYM [22] revealed that the optimized structures belong to space group *Pm* (no. 6). The atomic coordinates are given in Tables 4 and 5. It has to be noted that the number of atoms has more than doubled compared to Tables 2 and 3 due to symmetry reduction.

It also has to be noted that structure refinements based on these optimized atomic coordinates did not improve the quality of the fits. It must therefore be concluded that the crystal structures of **1** and **2** cannot be described well with fixed atomic positions and simple models of the atomic displacements.

The electronic band gaps of **1** and **2** calculated with PW1PW after geometry optimization are 1.04 and 1.33 eV, respectively. This is in accordance with the observed dark grey color of the powders.

The Projected Density of States was calculated for the optimized structures of **1** and **2** in space group 6 (Figure 4). In both compounds the highest valence states are mainly formed by copper and sulfur orbitals, while the lowest conduction bands

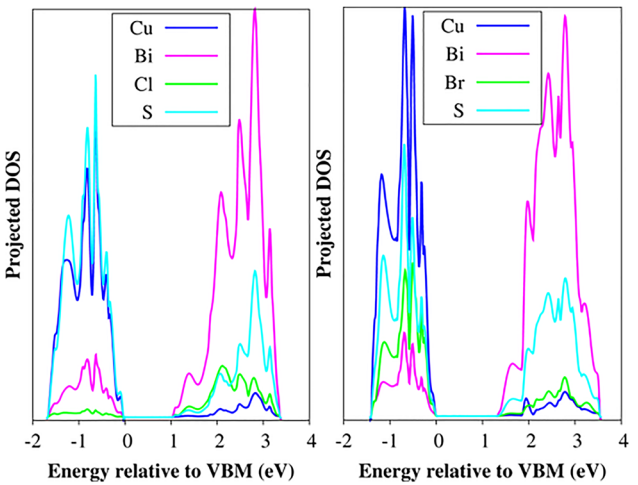

Figure 4: Projected density of states calculated with PW1PW for $CuBi_2S_3Cl$ (left) and $CuBi_2S_3Br$ (right). Orbital energies are given relative to the valence band maximum (VBM) in eV.

are predominantly composed of bismuth orbitals. The main difference between $CuBi_2S_3Cl$ and $CuBi_2S_3Br$ is the significantly larger contribution of bromide orbitals to the upper part of the valence band compared to chloride.

3 Conclusions

We presented the mechanochemical synthesis of two new quaternary copper bismuth sulfide halides, $CuBi_2S_3Cl$ (**1**) and $CuBi_2S_3Br$ (**2**). The crystal structures were refined in space group *C*2/*m* (no. 12) with satisfactory *R* values only if copper atoms are assumed to be disordered. Quantum-chemical calculations suggest a space group of lower symmetry for both compounds, *Pm* (no. 6). Refinements with theoretically optimized atomic coordinates did not lead to improvements of the *R* values. We therefore conclude that the crystal structures of (including the static disorder of the copper atoms in) **1** and **2** cannot be adequately modeled with fixed atomic positions and simple models of atomic displacement (isotropic displacement parameters). In particular, the copper atoms are assumed to be mobile at synthesis conditions. A better theoretical description should therefore be obtained by large supercells with a pseudorandom distribution of copper. However, this is beyond the scope of the present paper and will be addressed in a forthcoming study.

4 Experimental section

4.1 Synthesis of Bi_2S_3

Bismuth sulfide (Bi_2S_3) was synthesized mechanochemically by using the Fritsch Pulverisette 7 *classic line*, a high-energy planetary ball mill. Bismuth pellets (99.9%, Fluka) and sulfur (99.999%, Fluka) were filled into a 45 mL steel vessel in stoichiometric amounts and then milled for 2 h at 450 rpm. After 1 h of milling, the machine was paused for an hour to avoid overheating. The product was obtained as a metallic grey powder. The completion of the reaction was secured by powder X-ray diffraction measurements.

4.2 Synthesis of $CuBi_2S_3Cl$ (1) and $CuBi_2S_3Br$ (2)

$CuBi_2S_3Cl$ and $CuBi_2S_3Br$ were synthesized by using the Fritsch Pulverisette 7 *classic line*. The corresponding copper halide (CuCl, 99.9%, Sigma Aldrich, for **1**; or CuBr, 99.999%, Sigma Aldrich, for **2**) and bismuth sulfide were mixed in a 1:1 ratio in a 12 mL steel vessel equipped with six steel balls (diameter of 1 cm). Milling was carried out with 450 rpm, the milling time added up to a total of 4 h with 30-min breaks after 1 h of milling to avoid overheating of the machine. The ground products were tempered in a tube furnace under an argon atmosphere with a flow rate of 5 L h^{-1} at 200 °C for 3 h. Both products were obtained as dark grey powders. Results of the EDX measurements are shown in Table 6.

4.3 X-ray diffraction

Diffraction data was collected using a Rigaku SmartLab 3 kW diffractometer with CuKα radiation in Bragg-Bretano geometry. The diffractograms were measured over an angular range of 10°–120° with a scan rate of 0.2°/min for **1** and 0.5°/min for **2**.

The program Jana2006 and its implemented programs were used for leBail fit and Rietveld refinement. The model of $Cu_{1.5}Bi_{2.64}S_{3.42}Br_{2.58}$ [13] was used as a structure proposal. After leBail fit the refinement was continued using a pseudo-Voigt function to fit the peak profiles. Displacement and transparency corrections, asymmetry correction according to Berar-Baldinozzi [23] and roughness correction according to Pitschke, Herrmann and Mattern [24] were applied. The program Diamond 4.6 was used for graphical representation [25].

Table 6: Results of the EDX analyses for $CuBi_2S_3Cl$ and $CuBi_2S_3Br$.

$CuBi_2S_3Cl$	Calculated at-%	Measured at-%	$CuBi_2S_3Br$	Calculated at-%	Measured at-%
Cu	14.3	14.9	Cu	14.3	16.1
Bi	28.6	29.0	Bi	28.6	27.9
S	42.9	42.7	S	42.9	41.4
Cl	14.3	13.4	Br	14.3	14.6

Further details of the crystal structure investigation may be obtained from Fachinformationszentrum Karlsruhe, 76344 Eggenstein-Leopoldshafen, Germany (fax: +49-7247-808-259; E-mail: helpdesk@fiz-karlsruhe.de, https://www.ccdc.cam.ac.uk/structures/) on quoting the deposition number CSD-2105970 for $CuBi_2S_3Cl$ and CSD-2105969 for $CuBi_2S_3Br$.

4.4 EDX measurements

EDX measurements were carried out at the *Zentraleinrichtung Elektronenmikroskopie* (TU Berlin) on a ZEISS GeminiSEM500 NanoVP with a Bruker Quantax XFlash 6|60 detector and a stimulation energy of 15 keV. For the phase composition determination a device error of 5% is presumed.

4.5 Computational setup

The periodic DFT calculations were performed with CRYSTAL17 [26]. The hybrid functional PW1PW [27] was applied since it has shown good performance for the calculation of structural, electronic and energetic properties of solid oxides [28]. The wavefunctions were described with the recently developed BSSE-corrected atomic POB-TZVP-rev2 basis sets [29, 30]. Long-range London dispersion was taken into account by means of the DFT-D3(BJ) method [31, 32]. Based on our experience with other oxides, we reduced the s_8 parameter to 1.5363. Integral tolerances TOLINTEG were set to strict values 10^{-7}, 10^{-7}, 10^{-7}, 10^{-14}, 10^{-42}. A $2 \times 6 \times 4$ Monkhorst-Pack k-point grid was applied for the calculations of the conventional unit cells.

Acknowledgments: We thank Dr. Christoph Fahrenson from the *Zentraleinrichtung Elektronenmikroskopie* (ZELMI) for EDX measurements.
Author contributions: All the authors have accepted responsibility for the entire content of this submitted manuscript and approved submission.
Research funding: None declared.
Conflict of interest statement: The authors declare no conflicts of interest regarding this article.

References

1. Ruck M. *Z. Anorg. Allg. Chem.* 2002, *628*, 1537–1540.
2. Poudeu P. F., Ruck M. *J. Solid State Chem.* 2006, *179*, 3636–3644.
3. Poudeu Poudeu P. F., Söhnel T., Ruck M. *Z. Anorg. Allg. Chem.* 2004, *630*, 1276–1285.
4. Ruck M. *Z. Anorg. Allg. Chem.* 2002, *628*, 453–457.
5. Ruck M., Poudeu Poudeu P. F., Söhnel T. *Z. Anorg. Allg. Chem.* 2004, *630*, 63–67.
6. Heerwig A., Isaeva A., Ruck M. *Z. Anorg. Allg. Chem.* 2011, *637*, 1131–1136.
7. Heerwig A., Ruck M. *Z. Anorg. Allg. Chem.* 2011, *637*, 1814–1817.
8. Heerwig A., Merkle R., Maier J., Ruck M. *J. Solid State Chem.* 2011, *184*, 191–198.
9. Heerwig A., Müller U., Nitsche F., Ruck M. *Z. Anorg. Allg. Chem.* 2012, *638*, 1462–1467.
10. Heerwig A., Nitsche F., Ruck M. *Z. Anorg. Allg. Chem.* 2011, *637*, 62–66.

11. Heerwig A., Ruck M. *Z. Anorg. Allg. Chem.* 2009, *635*, 2162–2169.
12. Heerwig A., Ruck M. *Z. Anorg. Allg. Chem.* 2010, *636*, 1860–1864.
13. Heerwig A., Thybaut C. L. J., Ruck M. *Z. Anorg. Allg. Chem.* 2010, *636*, 2433–2438.
14. Balić-Zunić T., Mariolacos K., Friese K., Makovicky E. *Acta Crystallogr. Sect. B Struct. Sci.* 2005, *61*, 239–245.
15. Lewis J., Jr, Kupcík V. *Acta Crystallogr. Sect. B Struct. Sci.* 1974, *30*, 848–852.
16. Mariolacos K., Kupcík V. *Acta Crystallogr. Sect. B Struct. Sci.* 1975, *31*, 1762–1763.
17. Liang L.-C., Bilc D. I., Manoli M., Chang W.-Y., Lin W.-F., Kyratsi T., Hsu K.-F. *J. Solid State Chem.* 2016, *234*, 1–8.
18. Petříček V., Dušek M., Palatinus L. *Z. Kristallogr.* 2014, *229*, 345–352.
19. Palatinus L., Chapuis G. *J. Appl. Crystallogr.* 2007, *40*, 786–790.
20. Rietveld H. M. *J. Appl. Crystallogr.* 1969, *2*, 65–71.
21. Remy-Speckmann I., Bredow T., Lerch M. *Z. Naturforsch, B: Chem. Sci.* 2020, *75*, 921–925.
22. Stokes H. T., Hatch D. M. *J. Appl. Crystallogr.* 2005, *38*, 237–238.
23. Berar J.-F-, Baldinozzi G. *J. Appl. Crystallogr.* 1993, *26*, 128–129.
24. Pitschke W., Hermann H., Mattern N. *Powder Diffr.* 1993, *8*, 74–83.
25. Putz K. B. H. *Diamond – Crystal and Molecular Structure Visualization*. http://www.crystalimpact.com/diamond.
26. Dovesi R., Erba A., Orlando R., Zicovich-Wilson C. M., Civalleri B., Maschio L., Rérat M., Casassa S., Baima J., Salustro S., Kirtman B. *WIREs Comput. Mol. Sci.* 2018, *8*, e1360.
27. Bredow T., Gerson A. R. *Phys. Rev. B* 2000, *61*, 5194–5201.
28. Islam M. M., Maslyuk V. V., Bredow T., Minot C. *J. Phys. Chem. B* 2005, *109*, 13597–13604.
29. Vilela Oliveira D., Laun J., Peintinger M. F., Bredow T. *J. Comput. Chem.* 2019, *40*, 2364–2376.
30. Laun J., Bredow T. *J. Comput. Chem.* 2021, *42*, 1064–1072.
31. Grimme S., Antony J., Ehrlich S., Krieg H. *J. Chem. Phys.* 2010, *132*, 154104.
32. Grimme S., Ehrlich S., Goerigk L. *J. Comput. Chem.* 2011, *32*, 1456–1465.